11th World Congress on Structural and Multidisciplinary Optimisation
07th -12th, June 2015, Sydney Australia

Topology and Size Optimization of Modular Ribs in Aircraft Wings

A.Rinku[1], G K Ananthasuresh[2]
[1]PhD Student, Department of Mechanical Engineering, Indian Institute of Science & Principal Scientist, National Aerospace Laboratories, Bengaluru, India, rinku@ccadd.cmmacs.ernet.in
[2]Professor, Department of Mechanical Engineering, Indian Institute of Science, Bengaluru, India, suresh@mecheng.iisc.ernet.in

1. Abstract
Semi-monocoque construction currently followed for ribs with full-depth web in aircraft wings requires extensive elastic analysis to ensure adequate stiffness, strength, and stability against local buckling while reducing the weight. In this work, we address this problem by developing a modular design enabled by fewer components as compared to current design. As a result, the cost and complexity of manufacturing the components as well as the overall assembly reduce. Furthermore, the design process of the overall wing becomes computationally efficient. Optimality is achieved by topology and size optimization techniques. A systematic three-stage procedure for rib design for any given aircraft wing is developed and is demonstrated using the wing of a light transport aircraft.

Keywords
Design optimization, Topology-Optimization, Wing ribs, Modular design.

2. Introduction
There are several successful examples of application of topology optimization in optimal aircraft structural design. Balabanov and Haftka [1] represented the internal structure of a wing as a truss and optimized the cross-sectional area of the ground structure of the interconnected truss elements. In the A380 project of Airbus Industries, topology optimization was used to obtain new and lighter component designs such as the inboard outer fixed leading-edge ribs and the fuselage door intercostals. This has contributed weight savings on the order of 1000 kg per aircraft [2]. The successful engineering practices of the topology optimization are due to intense research in this field [3-10]. Locatelli et al. [11] proposed a new design concept in wing-box design called “Sparibs” by using topology and sizing optimization techniques, instead of using the classic design concept of straight spars and ribs. Wang et al. [12] proposed a topology optimization method which is based on the subset simulation method used in reliability analysis on improving the computational efficiency. They demonstrated this technique in optimizing the wing leading edge ribs and were able reduce the weight of the rib by 18.4%.

In this work, we propose a modular design of wing-ribs with fewer components than conventional semi-monocoque design (web reinforced with stiffeners), which is likely to lower the cost of manufacturing and assembly. Furthermore, the design process of the overall wing becomes computationally efficient. Optimality is achieved by topology and size optimisation techniques. A systematic three-stage procedure is developed and demonstrated on a typical light transport aircraft wing ribs.

3. Optimization of wing ribs
A typical Light transport aircraft (LTA) wing under consideration is of two-spar construction, with 23 rib stations per side of the wing. At each rib station, the rib is divided into three portions, viz., Nose rib, Inter spar (I/S) rib, and trailing edge rib. This paper deals with optimization of I/S ribs. A typical LTA wing is shown in Fig.1a and conventional semi-monocoque rib design is shown in Fig. 1b, in which the web is reinforced with vertical stiffeners to resist the loads acting on the rib and to avoid buckling. The optimization procedure is explained next.

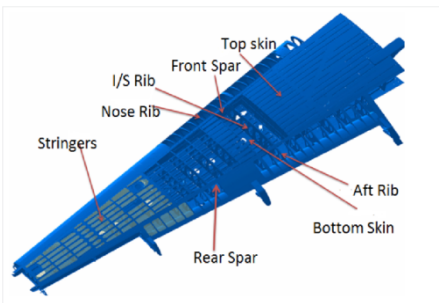

Figure 1a: Typical Light Transport Aircraft wing

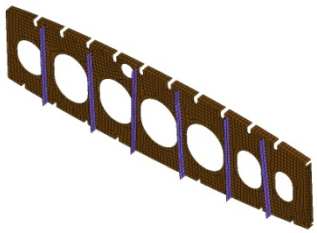

Figure 1b: Typical conventional semi-monocoque rib

4. **Optimization Framework**

The three stages in the proposed design procedure include two stages of optimization followed by modular design of the rib as shown in Fig. 2. Step 1 involves topology optimization of a few selected ribs where mean compliance is minimized subject to the volume constraint. As the loads and lengths of the ribs are proportional to the chord, the pattern repeatability of the internal structure was achieved by maintaining the same area-ratio between design and non-design areas for all the ribs. The non-design material region exist all along the periphery of the I/S ribs.

Step 2 involves size optimization of the ribs obtained through topology optimization done in the first step. The objective here is to minimize the mass subject to stress and buckling constraints. Each topology-optimized rib is thus improved by determining the cross-section dimensions of the beam segments in the rib.

Step 3 is the modular design of the intermediate ribs. As the pattern repeatability is achieved through topology optimization, the internal members of the rib can be located proportionally as per the chord-length using non-dimensional analysis. Non-dimensional stiffness, stress, and other parameters [13] help design any intermediate rib with standard available beam segments by maintaining the area and the moment of inertia.

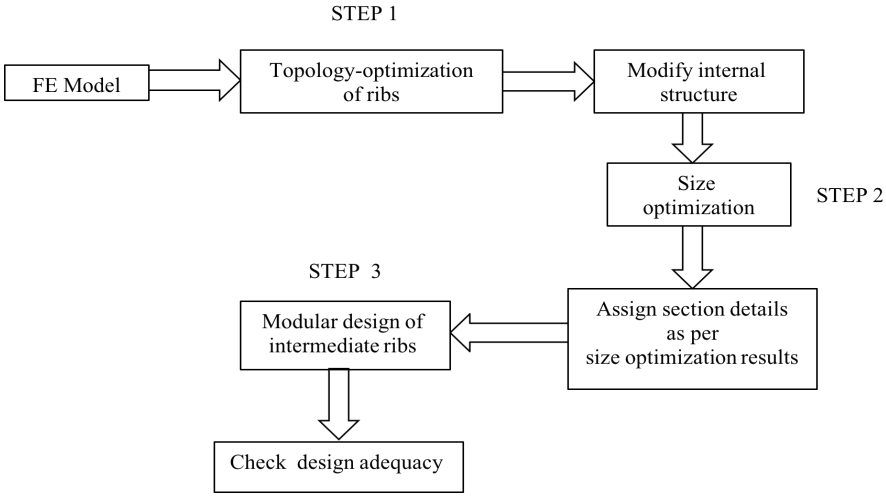

Figure 2: Three-step optimization framework for rib design aircraft wings

4.1 Topology optimization of wing ribs

Topology optimization was carried out on a few arbitrarily selected I/S ribs; Rib no. 8,12, 16 and 19 as shown in Fig. 3.The objective function is to minimize the strain energy (SE) with the constraint on volume . This can be stated in the discretized finite element framework as follows:

$$\begin{aligned} \min_{\boldsymbol{x}} SE &= \frac{1}{2}\boldsymbol{u}^T\boldsymbol{k}\boldsymbol{u} = \frac{1}{2}\sum_{i=1}^{n} x_i^{\rho} u_i^T k_i u_i \\ \boldsymbol{k}\boldsymbol{u} &= \boldsymbol{f} \\ \frac{V}{V_0} &= 0.3 \\ \boldsymbol{x} &= \{x_1, x_2, \dots\dots, x_n\}^T \\ 0 < x_{min} &\le x_i \le 1 \quad (i = 1, \dots, n) \end{aligned} \tag{1}$$

where $\boldsymbol{u}$ is the global displacement vector of size $n\times1$, $\boldsymbol{k}$ the global stiffness matrix , $\boldsymbol{f}$ the external load vector, V_0 the initial volume, V the final volume, and x_i the i^{th} element's density that indicates the presence or absence of the material in the corresponding element..

Topology optimization was carried out using commercial software Altair Optistruct. The ribs were analyzed as continuum structure using 2D finite elements CQUAD4 and CTRIA3. The aim of this step is to obtain optimum distribution of material and to achieve pattern repeatability in the rib geometry. The chord-wise load distribution was computed using *panel code* by the aerodynamic group at the National Aerospace Laboratories, Bengaluru [14] on the top and bottom wing surfaces for V_D (Dive Speed) case at the selected rib locations shown in Fig. 4. As can be seen in the figure, the loads are proportional to the local chord. Portions of the rib at the top, bottom and sides are defined as non-design space to accommodate the stringer cut-outs and attachments to spars.

With the rib loads and lengths being proportional to the local chord and by maintaining the same ratio between design space area (A_DS) and total rib area (A_Tot) for all the ribs as shown in Fig. 5, the topology optimization results are shown in Fig. 6. In this, the red colour indicates presence of the material and blue colour the void regions. It is evident that there is pattern repeatability in the rib structure which points to generalized rib

geometry shown in Fig. 7. The general rib geometry shown in Fig. 7 also indicates the dimensions required to construct any intermediate rib in the wing. In Fig. 7, "*l1, 12, l3 ,l4 ,l5, l6"* indicates the lengths of the inclined members and " a, b, c, d, e, f, g, h" indicates the intersection points of the inclined members with top flange , bottom flange , front spar and rear spar, which are measured from front spar top (Ft). These dimensions can be mentioned in terms of % chord in relation to the rib location (% span) as shown in Fig. 8. With this non-dimensional graph, it is possible to define geometry of any intermediate rib.

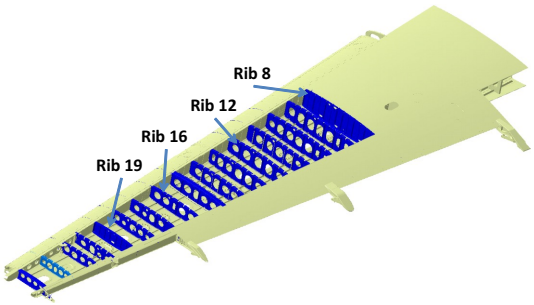

Figure 3. Typical LTA wing with conventional Rib design

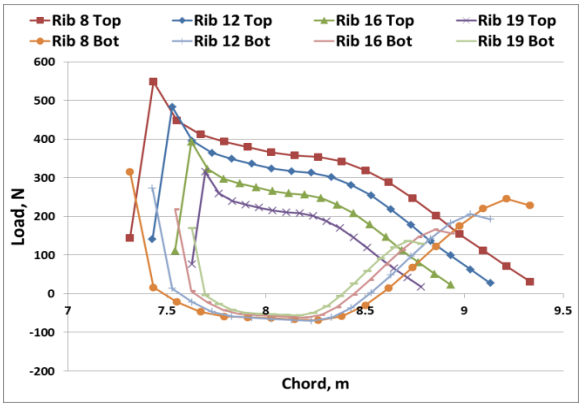

Figure 4: Chord wise load distribution

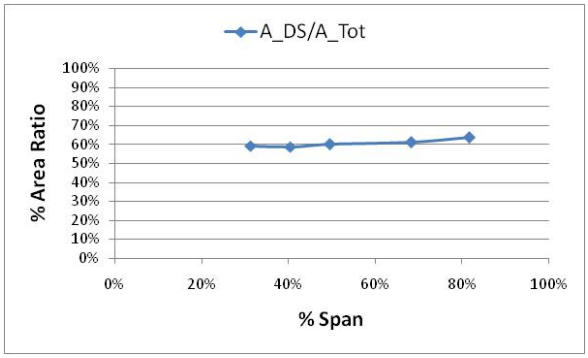

Figure 5: Area Ratio

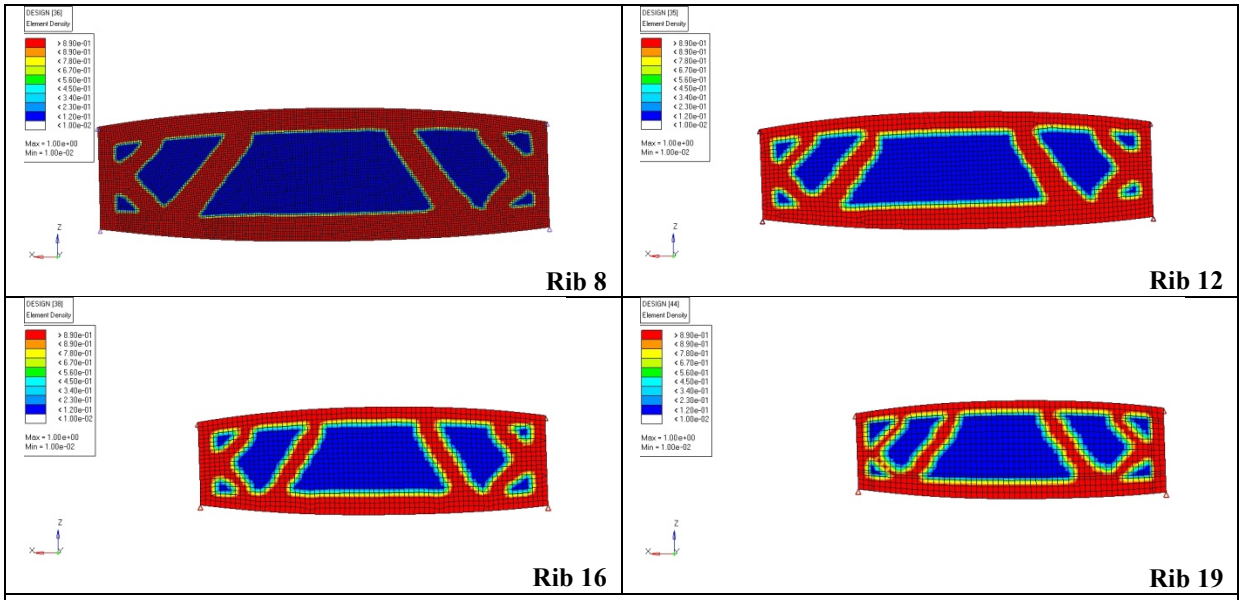

Figure 6 : Topology optimization plots for Rib 8,12,16 and 19

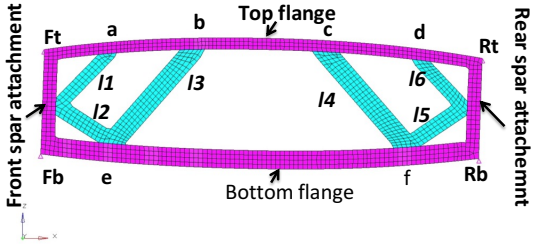

Figure 7: Generalized Rib geometry

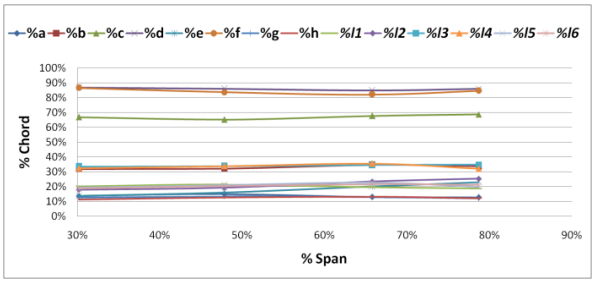

Figure 8: Non dimensional plot of Rib geometry

4.2. Size optimization of the wing ribs

Step 2 involves size optimization of the topology optimized ribs for minimizing the mass (M) with stress (σ_{max}) and buckling constraints (Buckling factor, BF). A typical buckling constraint is a lower bound of 1.0 indicating that the structure is not to buckle under the given static load. Each topology optimized rib was subjected to size optimization to get thicknesses of various internal elements of the rib. This problem can be formulated as follows:

$$\begin{gathered} \min_{T} M \\ \sigma_{max} \ll 265\ MPa \\ 1 - BF \leq 1 \\ 0.8 \leq T \leq 5 \end{gathered} \qquad (2)$$

Size optimization was carried out on ribs 8, 12, 16, and 19 using Altair Optistruct. With the optimum thickness values and corresponding widths of the various elements of the rib, area (A) and Moment of inertia (MI) values were computed for each element and plotted with respect to % span. Typical graphs are shown Figs. 9 and 10 for the bottom flange. By using these graphs, cross section of any intermediate rib can be defined, as explained next.

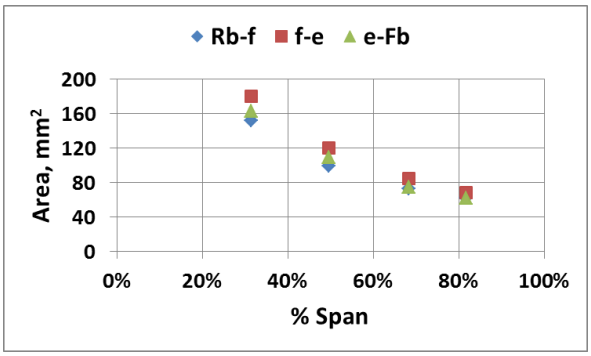

Figure 9: Cross sectional area graph for bottom flange

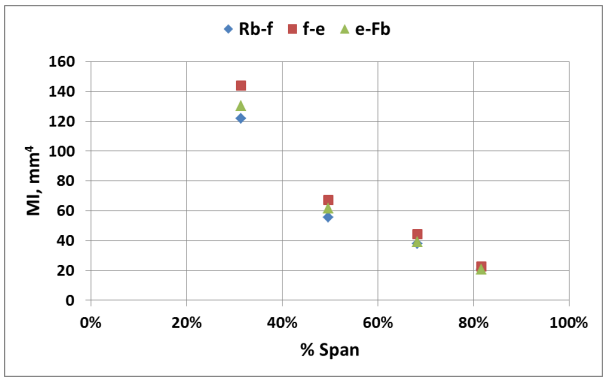

Figure 10: Moment of inertia graph for bottom flange

4.3. Modular design of intermediate ribs

Step 3 is modular design of the intermediate ribs. As the pattern repeatability is achieved through topology optimization, internal structure of any intermediate rib can be obtained by using non-dimensional plot of rib geometry shown in Fig. 8. Cross sectional details obtained from the topology and size optimization process, it is possible to decide the cross section detail of any intermediate rib by selecting the standard available section by maintaining the area and moment of inertia values obtained from the optimization (Figs. 9, 10).

To demonstrate this process an intermediate rib 10 is considered. Its internal structures can be obtained from the Fig. 8 by locating the rib at its span wise location (39%). Once the rib internal structure is obtained, its cross sectional area can be decided by using Area and MI graphs. We can choose a suitable standard section which meets cross sectional requirements and local crippling criteria. In this case, we have selected a channel section to check the design adequacy. Linear static and buckling analysis were carried out using Altair Optistruct and the results are shown in Table 1. The geometry of rib 10 with modular design concept is shown Figs. 11 and 12. Fig. 12 shows the geometry of the rib with stringer cut-outs as per the practical design requirement.

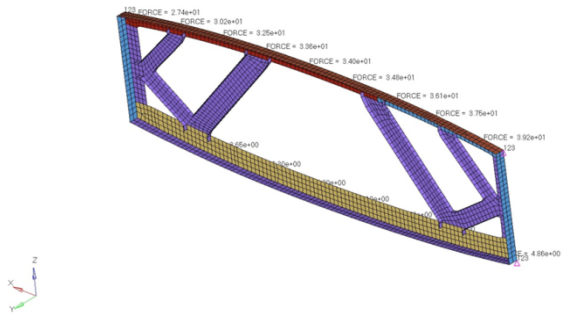

Figure 11: Modular design of rib 10 (without stringer cut-out)

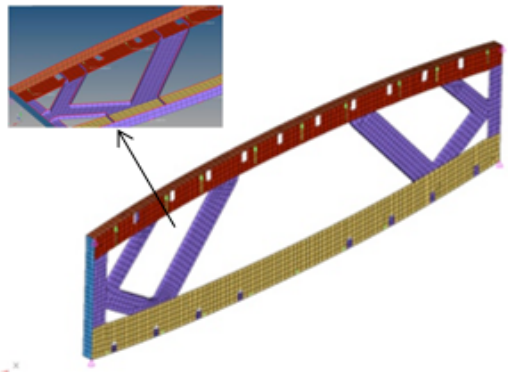

Figure 12: Modular design of rib 10 (with stringer cut-out)

To prove the efficiency of the modular design procedure, we have compared the results of modular design with the two-step optimization procedure and conventional rib design. The conventional rib design is shown in Fig.13, which contains full depth web, with lightening holes and stiffeners at regular interval to meet the buckling requirements. Size optimization was carried out on this rib with stress and buckling constraints and the results are shown in Table 1.

The rib was optimized using two-step optimization procedure comprising topology optimization followed by size optimization. The topology optimization result is shown in Fig. 14, where it can be seen that it is very much similar to the modular design obtained using Fig. 8. Next, size optimization was carried out to meet buckling and stress requirements whose results are shown in Table 1.

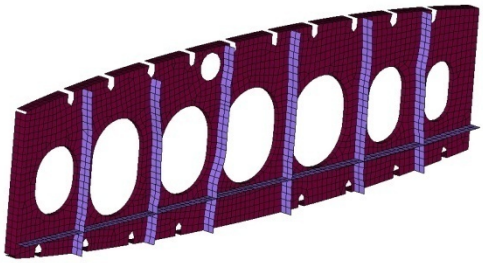

Figure 13 : Conventional design of Rib 10

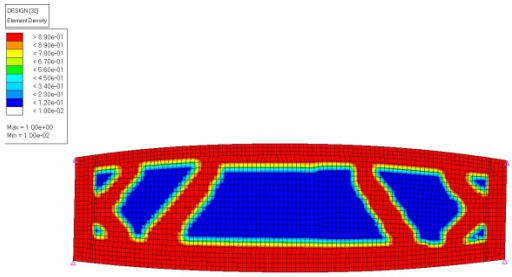

Figure 14 : Topology optimization plot for Rib 10

Table 1: Results of Rib 10 Optimization

Rib 10		Weight(Kg)	Max Deflection (mm)	Stress (MPa)	Buckling factor
Modular design	Without stringer cut-out	0.7	0.4	60	4
	With stringer cut-out	0.76	0.39	70.6	3.23
Conventional rib design		0.974	0.42	45	1
Two-step optimization (Without stringer cut-out)		0.68	0.35	63	1

4.4. Discussion

Results of modular design, two-step optimization procedure, and conventional design are shown in Table 1. A rib designed with two-step optimization procedure is 30% lighter as compared to the conventional rib design for the same buckling factor. The modular rib design is 22% lighter as compared to conventional design with three times more buckling factor. The two step optimization process and the modular design concept proposed in this paper results in much lighter structure as compared to conventional design. Even though von Mises stress is more in the proposed modular design as compared to conventional design, the absolute value is much less than the maximum allowable stress of 265 MPa. The complete wing with modular rib design is shown in Fig. 15.

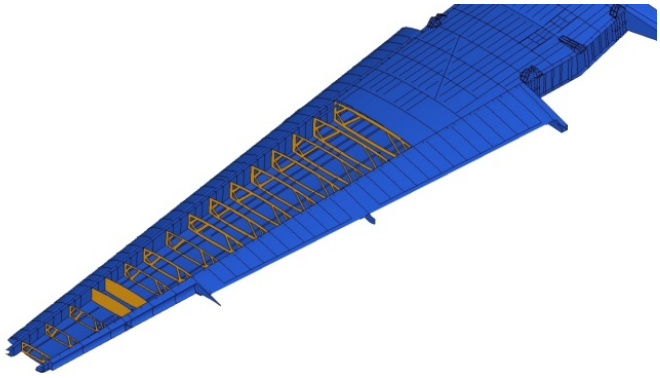

Figure 15. Typical Light transport aircraft wing with modular Ribs

5. Conclusion

The modular rib design is "satisficing" in nature in that it satisfies all the design and manufacturing requirements but is only nearly optimal. However, the unique feature of this procedure is the modular design wherein the internal members of all the ribs are decided as per their position in the wing. As a result, the design is amenable for economical manufacturing. Through an example, it is proved that the new design procedure is more efficient as compared to current practices in terms of weight and performance.

6. Acknowledgments

Authors thank Dr. Vidyadhar Mudkavi, Head, CTFD, CSIR-NAL, for his support and encouragement. Also thank Director, CSIR-NAL and Head, C-CADD, CSIR-NAL for granting permission to carry out the work.

7. References

1. Balabanov V O, Haftka R T, Topology optimization of transport wing internal structure, Journal of Aircraft, 33(1), 232-233, 1996.
2. Krog L, Tucker A, Kamp M, Boyd R., "Topology Optimization of Aircraft Wing Box Ribs," *The Altair Technology Conference 2004,* Vol. 6, Altair Engineering, Troy, MI, 2004, pp. 1-16.
3. Bendsøe M P, Kikuchi N, "Generating Optimal Topologies in Structural Design Using Homogenization," *Computer Methods in Applied Mechanics and Engineering,* Vol. 71, 1988, pp. 197-224.
4. Bendsøe M P, "Optimal Shape Design as a Material Distribution Problem," *Structural and Multidisciplinary Optimization,* Vol. 1, No. 4, 1989, pp. 193-202.
5. Zhou M, Rozvany G I N, "The Coc Algorithm, Part II: Topological, Geometry and Generalized Shape Optimization," *Computer Methods in Applied Mechanics and Engineering,* Vol. 89, Nos. 1-3, 1991, pp. 309-336.
6. Sigmund O, "A 99 Line Topology Optimization Code Written in Matlab," *Structural and Multidisciplinary Optimization,* Vol. 21, No. 2, 2001, pp. 120-127.
7. Svanberg K, "The Method of Moving Asymptotes: A New Method for Structural Optimization," *International Journal for Numerical Methods in Engineering,* Vol. 24, 1987, pp. 359-373.
8. Bruggi M, Duysinx P, Topology optimization for minimum weight with compliance and stress constraints. *Structural and Multidisciplinary Optimization* (2012).
9. Kočvara M, Stingl M, Solving stress constrained problems in topology and material optimization, *Structural and Multidisciplinary Optimization*, January 2012.
10. Sigmund O, Maute K, Topology optimization approaches .A comparative review, *Structural and Multidisciplinary Optimization* (2013) 48:1031–1055.
11. Locatelli D, Mulani S B, Kapania R K, Wing-Box Weight Optimization Using Curvilinear Spars and Ribs (SpaRibs), Journal of Aircraft, Vol. 48, No. 5, September-October 2011.
12. Wang Q, Lu Z, Zhou C, New Topology Optimization Method for Wing Leading-Edge Rib, Journal of Aircraft, Vol. 48, No. 5, September-October 2011.
13. Bhargav S. D. B., Varma H. I., and Ananthasuresh G. K., Non-dimensional Kinetoelastostatic Maps for Compliant Mechanisms*, Proc. ASME 2013 International Design Engineering Technical Conferences*, August 4-7, 2013, Portland, Oregon, USA, Paper no. DETC2013-12178.
14. Internal report, C-CADD, National Aerospace Laboratories, Bengaluru, India.